

Neutrinos as a diagnostic of cosmic ray galactic-extragalactic transitionMarkus Ahlers,¹ Luis A. Anchordoqui,² Haim Goldberg,² Francis Halzen,³ Andreas Ringwald,¹ and Thomas J. Weiler⁴¹*Deutsches Elektronen-Synchrotron DESY, Hamburg, Germany*²*Department of Physics, Northeastern University, Boston, Massachusetts 02115, USA*³*Department of Physics, University of Wisconsin, Madison Wisconsin 53706, USA*⁴*Department of Physics and Astronomy, Vanderbilt University, Nashville Tennessee 37235, USA*

(Received 12 May 2005; published 1 July 2005)

Motivated by a recent change in viewing the onset of the extragalactic component in the cosmic ray spectrum, we have fitted the observed data down to $10^{8.6}$ GeV and have obtained the corresponding power emissivity. This transition energy is well below the threshold for resonant $p\gamma$ absorption on the cosmic microwave background, and thus source evolution is an essential ingredient in the fitting procedure. Two-parameter fits in the spectral and redshift evolution indices show that a standard Fermi E_i^{-2} source spectrum is excluded at larger than 95% confidence level (CL). Armed with the primordial emissivity, we follow Waxman and Bahcall to derive the associated neutrino flux on the basis of optically thin sources. For pp interactions as the generating mechanism, the neutrino flux exceeds the AMANDA-B10 90% CL upper limits. In the case of $p\gamma$ dominance, the flux is consistent with AMANDA-B10 data. In the new scenario the source neutrino flux is considerably enhanced, especially below 10^9 GeV. Should data from AMANDA-II prove consistent with the model, we show that IceCube can measure the characteristic power law of the neutrino spectrum, and thus provide a window on the source dynamics.

DOI: [10.1103/PhysRevD.72.023001](https://doi.org/10.1103/PhysRevD.72.023001)

PACS numbers: 96.40.-z, 98.70.Sa, 95.85.Ry

I. INTRODUCTION

A plethora of explanations have been proposed to address the production mechanism of ultra-high energy cosmic rays [1]. In the absence of a single model which is consistent with all data, the origin of these particles remains a mystery. Clues to solve the mystery are not immediately forthcoming from the data, particularly since various experiments report mutually inconsistent results. In recent years, a somewhat confused picture regarding the energy spectrum and arrival direction distribution has been emerging. Since 1998, the AGASA Collaboration has consistently reported [2] a continuation of the spectrum beyond the expected Greisen–Zatsepin–Kuzmin (GZK) cutoff [3], which should arise at about $10^{10.7}$ GeV if cosmic ray sources are at cosmological distances. In contrast, the most recent results from HiRes [4] describe a spectrum which is consistent with the expected GZK feature. This situation exposes the challenge posed by systematic errors in these types of measurements. Further confusing the issue, the AGASA Collaboration reports observations of event clusters which have a chance probability smaller than 1% to arise from a random distribution [5], whereas the recent analysis reported by the HiRes Collaboration showed that their data are consistent with no clustering among the highest energy events [6].

Deepening the mystery, recent HiRes data have been interpreted as a change in cosmic ray composition, from heavy nuclei to protons, at $\sim 10^9$ GeV [7]. This is an order of magnitude lower in energy than the previous crossover deduced from the Fly's Eye data [8]. The endpoint of the galactic flux is expected to be dominated by iron, as the large charge Ze of heavy nuclei reduces their Larmor radius (containment scales linearly with Z) and facilitates

their acceleration to highest energy (again scaling linearly with Z). The dominance of nuclei in the high energy region of the Galactic flux carries the implication that any change-over to protons represents the onset of dominance by an extragalactic component. The inference from this new HiRes data is therefore that the extragalactic flux is beginning to dominate the galactic flux already at $\sim 10^9$ GeV. Significantly, this is well below $E_{\text{GZK}} \sim 10^{10.7}$ GeV [3], the threshold energy for resonant $p\gamma_{\text{CMB}} \rightarrow \Delta^+ \rightarrow N\pi$ energy-loss on the cosmic microwave background (CMB), and so the extragalactic flux samples sources even at high redshift.

The dominance of extragalactic protons at lower energy can be consistent with recently corroborated structures in the cosmic ray spectrum. A second knee, recognized originally in AGASA data [9], is now confirmed by the HiRes-MIA Collaboration [10]. At $10^{8.6}$ GeV, the energy spectrum steepens from E^{-3} to $E^{-3.3}$. This steepening at the second knee can be explained [11] by energy losses of extragalactic protons over cosmic distances, due to e^+e^- pair-production on the CMB. The theoretical threshold of the energy-loss feature occurs at $10^{8.6}$ GeV, and therefore allows for proton dominance even below this energy. However, the HiRes data [7] seem to indicate a composition change coincident with the energy of the second knee (from about 50% protons just below to 80% protons just above), and therefore argues for the beginning of extragalactic proton dominance at the second knee. Another feature in the cosmic ray spectrum is the ankle at $\sim 10^{10}$ GeV where the spectrum flattens from $E^{-3.3}$ to $E^{-2.7}$. This has been commonly identified with the onset of the extragalactic flux in the past. In the aftermath of the new HiRes data, the ankle can now be

interpreted as the minimum in the e^+e^- energy-loss feature.

These changes in viewing the onset of the extragalactic component have spurred a refitting of the cosmic ray data down to $10^{8.6}$ GeV with appropriate propagation functions and extragalactic injection spectra [11,12]. The major result is that the injection spectrum is significantly steeper than the standard E_i^{-2} predicted by Fermi engines. This result has consequences for neutrino observation: predictions for both the cosmogenic fluxes (produced via interactions of super-GZK cosmic-rays on the CMB) and the direct neutrino luminosity from optically thin sources can be significantly modified. The implication for cosmogenic neutrinos has been discussed elsewhere [13,14]. In this paper we analyze the impact on neutrino luminosities from optically thin sources which are associated with this change in view of the galactic/extragalactic crossover energy.

The outline of the paper is as follows. We begin in Sec. II with an estimate of the power density of cosmic rays assuming a “low” energy onset of dominance by an extragalactic component. This is accomplished by a goodness-of-fit test of our scenario with the energy spectrum as observed by the Akeno [9] & AGASA [2] and the Fly’s Eye [8,15] & HiRes [4] experiments, respectively, in the energy range from the second knee upward, i.e., $10^{8.6}$ GeV $< E < 10^{11}$ GeV. In the fitting procedure we use appropriate propagation functions [16] that take into account photo-meson and pair production on the CMB. Armed with the cosmic ray emissivities required to populate the observed spectrum with extragalactic protons all the way down to $10^{8.6}$ GeV, in Sec. III we derive predictions of neutrino fluxes associated with $p\gamma$ or pp interactions in sources which are optically thin. To this end, we follow the procedure delineated by Waxman and Bahcall (WB) [17], but instead of assuming a specific cosmic ray injection spectrum $\propto E_i^{-2}$ and redshift source evolution $\propto (1+z)^3$, we use values for the spectral and source evolution indices complying with the best fits to the spectra obtained in Sec. II. In Sec. IV we review the computation of cosmogenic neutrinos and show that in the new low-energy crossover scenario, the associated neutrino spectra from optically thin sources dominates over the cosmogenic flux. In Sec. V we calculate event rates at IceCube [18] expected from source fluxes derived in Sec. III, and on this basis assess the potential of this detector to constrain the crossover energy between galactic and extragalactic dominance in the cosmic ray spectrum. Section VI contains a summary of our results and conclusions.

II. EXTRAGALACTIC COSMIC RAY POWER

It is helpful to envision the cosmic ray engines as machines where protons are accelerated and (possibly) permanently confined by the magnetic fields of the acceleration region. The production of neutrons and charged

pions and subsequent decay produces both neutrinos and cosmic rays: the former via $\pi^+ \rightarrow e^+ \nu_e \nu_\mu \bar{\nu}_\mu$ (and the conjugate process), the latter via neutron diffusion from the region of the confined protons. If the neutrino-emitting source also produces high energy cosmic rays, then pion production must be the principal agent for the high energy cutoff on the proton spectrum. Conversely, since the protons must undergo sufficient acceleration, inelastic pion production needs to be small below the cutoff energy; consequently, the plasma must be optically thin. Since the interaction time for protons is greatly increased over that of neutrons because of magnetic confinement, the neutrons escape before interacting, and on decay give rise to the observed cosmic ray flux. The foregoing can be summarized as three conditions on the characteristic nucleon interaction time scale τ_{int} ; the neutron decay lifetime τ_n ; the characteristic cycle time of confinement τ_{cycle} ; and the total proton confinement time τ_{conf} : (1) $\tau_{\text{int}} \gg \tau_{\text{cycle}}$; (2) $\tau_n > \tau_{\text{cycle}}$; (3) $\tau_{\text{int}} \ll \tau_{\text{conf}}$. The first condition ensures that the protons attain sufficient energy. Conditions (1) and (2) allow the neutrons to escape the source before decaying. Condition (3) permits sufficient interaction to produce neutrons and neutrinos. We take these three conditions together to define an optically thin source. A desirable property of this low-damping scenario is that a single source will produce cosmic rays with a smooth spectrum across a wide range of energy.

Assigning extragalactic dominance to energies beginning at $\sim 10^9$ GeV, rather than $\sim 10^{10}$ GeV, increases the required energy production rate of extragalactic cosmic rays. The power density in the energy range 10^{10} GeV to 10^{12} GeV is found to be $\dot{\epsilon}_{\text{CR}}[10^{10}, 10^{12}] \sim 5 \times 10^{44}$ erg Mpc $^{-3}$ yr $^{-1}$ [19]. As emphasized in [19], this result is independent of source evolution: for the stated energy interval, cosmic rays from distant sources will undergo significant energy losses on the CMB, and thus only nearby sources contribute to the observed spectrum. In what follows we obtain analogous power densities corresponding to the lower energy onset of extragalactic dominance. As can be expected, these will have sensitivity to source evolution.

We assume an isotropic distribution of neutron-emitting sources that can be described by a comoving luminosity distribution $\mathcal{L}_n(r, E_i)$, where E_i is the injection energy and r the distance to Earth. The number of protons N_p arriving at Earth with energy E per units of energy, area A , time t and solid angle Ω reads,

$$J_p \equiv \frac{d^4 N_p}{dE dA dt d\Omega} = \frac{1}{4\pi} \int_0^\infty dE_i \int_0^\infty dr \left| \frac{\partial P_{p|n}(E; E_i, r)}{\partial E} \right| \mathcal{L}_n \quad (1)$$

where $P_{p|n}$ is the propagation function introduced in Ref. [16] which gives the expected number of protons

above a threshold energy E if a neutron with energy E_i was emitted from a source at a distance r . The Monte Carlo program that computes P_{pln} uses SOPHIA [20] as an external package for simulation of the GZK interactions. The program exploits a continuous energy-loss approximation to describe the e^+e^- pair production process. To estimate the differential flux of protons, we calculate the P_{pln} function for infinitesimal steps (1–10 kpc) as a function of the redshift z and multiply the corresponding infinitesimal probabilities starting at a distance $r(z)$ down to Earth with $z = 0$.

We take all sources to have identical injection spectra $d\dot{N}_n/dE_i \propto E_i^{-\gamma}\Theta(E_{i,\max} - E_i)$, and parametrize the redshift evolution of the source luminosity and the comoving number density ρ_{CR} by a simple power law,

$$\mathcal{L}_n = \rho_{\text{CR}}[1 + z(r)]^n \Theta(z - z_{\min})\Theta(z_{\max} - z) \frac{d\dot{N}_n}{dE_i}, \quad (2)$$

where the redshift z and the distance r are related by $dz = (1+z)H(z)dr$. The Hubble expansion rate at a redshift z is related to the present one H_0 through $H^2(z) = H_0^2[\Omega_M(1+z)^3 + \Omega_\Lambda]$, where Ω_M and Ω_Λ are the matter and vacuum-energy densities in terms of the critical density. Here we take $\Omega_M = 0.3$ and $\Omega_\Lambda = 0.7$, in agreement with WMAP observations [21]. The results turn out to be rather insensitive to the precise values of the cosmological parameters within their uncertainties. The minimal and maximal redshift parameters z_{\min} and z_{\max} exclude the existence of nearby and early time sources. As a default value, we take $z_{\min} = 0.012$, corresponding to $r_{\min} = 50$ Mpc, and comment on the effect of possible variations where appropriate. Note that the effects due to a change in z_{\max} can be largely compensated by a change in n . Therefore, we fix $z_{\max} = 2$ in the following and study the dependences on n only. For the maximum injection energy we take as a default value $E_{i,\max} = 10^{12.5}$ GeV. Most of our results are insensitive to this choice, as long as $E_{i,\max}$ is above $\sim 10^{11.5}$ GeV (see also Ref. [13]), as we will see in the following.

The cosmic ray spectra as observed by Akeno [9] & AGASA [2] and Fly's Eye [8,15] & HiRes [4] are fitted and confidence levels are assigned using a Poisson likelihood following the procedure detailed in Ref. [13]. The 95% CL exclusion contours in the $n - \gamma$ plane for the two data samples are shown in Fig. 1. The parameters for the best fit, shown in Fig. 2, are given in Table I. The disparity in the goodness-of-fit tests of the two data samples is largely originating in the presence of a spurious bump in the region of $10^{9.4}$ GeV of the Akeno & AGASA data (cf. Ref. [13]). This in turn stems from combining the data of the Akeno array and the full AGASA experiment. Interestingly, *the new scenario with extragalactic cosmic rays dominating the spectrum below the ankle, down to the second knee at $E_- = 10^{8.6}$ GeV, is inconsistent at more than a 2σ level with standard Fermi engine models that suggest an injec-*

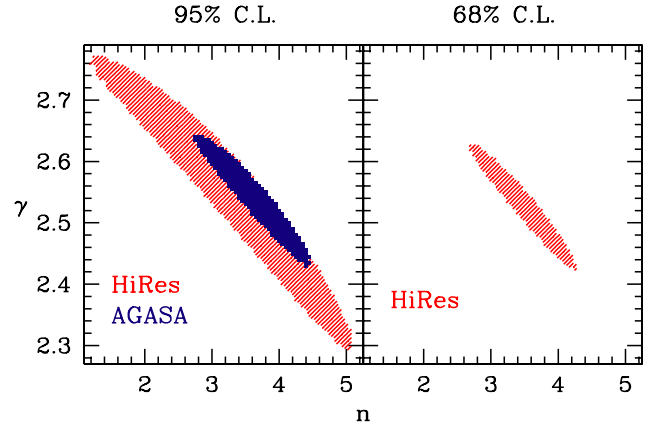


FIG. 1 (color online). The goodness-of-fit test of the low crossover scenario, using the method outlined in Ref. [13]. In the left panel we show the 95% CL allowed regions in the $n - \gamma$ plane, obtained with Fly's Eye & HiRes and Akeno & AGASA data. In the right panel we show the corresponding 68% CL obtained from Fly's Eye & HiRes data. In the fitting procedure we used data in the energy interval from $E_- = 10^{8.6}$ GeV to $E_+ = 10^{11}$ GeV, taking $z_{\min} = 0.012$ and $z_{\max} = 2$.

tion spectrum $\propto E_i^{-2}$. Note that for both data samples the best fit yields $\gamma = 2.54$. Additionally, $\gamma < 2.4$ is disfavored at the 1σ level by Fly's Eye [8,15] & HiRes [4] data and at the 2σ level by Akeno [9] & AGASA [2] data. We have checked that this is robust against variations of $z_{\min} \leq 0.012$ and $E_{i,\max} \geq 10^{11.3}$ GeV.

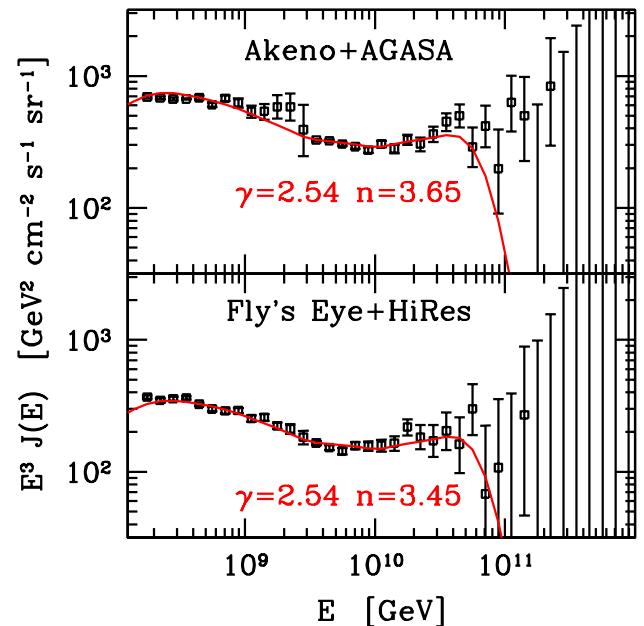


FIG. 2 (color online). Best fits to the ultra-high energy cosmic ray spectrum in the energy interval $[E_-, E_+]$ as observed by Akeno & AGASA and Fly's Eye & HiRes. We set $E_- = 10^{8.6}$ GeV, $E_+ = 10^{11}$ GeV, $z_{\min} = 0.012$, $z_{\max} = 2$, and $E_{i,\max} = 10^{12.5}$ GeV.

TABLE I. Best fit parameters

Experiment	γ	n	$\dot{\epsilon}_{\text{CR}}[10^{8.6} \text{ GeV}, 10^{12.5} \text{ GeV}]$
AGASA	2.54	3.65	$2.5 \times 10^{45} \text{ erg Mpc}^{-3} \text{ yr}^{-1}$
HiRes	2.54	3.45	$1.3 \times 10^{45} \text{ erg Mpc}^{-3} \text{ yr}^{-1}$

It is conceivable that the extragalactic proton flux largely exceeds the nearby data below $10^{8.6}$ GeV. As can be seen in Fig. 2, this is not the case for the best fit values. *Moreover, if we make a more sophisticated analysis with a galactic component below $10^{8.6}$ GeV, the 2σ allowed regions will shrink.*

At this stage, it is worthwhile to mention that we have verified the consistency of the simulations by fitting the data above 10^{10} GeV and comparing the cosmic ray power density,

$$\dot{\epsilon}_{\text{CR}}[E_{i,\text{min}}, E_{i,\text{max}}] = \rho_{\text{CR}} \int_{E_{i,\text{min}}}^{E_{i,\text{max}}} dE_i E_i \frac{d\dot{N}}{dE_i}, \quad (3)$$

with the result obtained in [19]. Our best fits, using Eq. (1) with $\gamma = 2$ and $n = 3$, correspond to $\dot{\epsilon}_{\text{CR}}[10^{10} \text{ GeV}, 10^{12} \text{ GeV}] = 4.8 \times 10^{44} \text{ erg Mpc}^{-3} \text{ yr}^{-1}$ and $\dot{\epsilon}_{\text{CR}}[10^{10} \text{ GeV}, 10^{12} \text{ GeV}] = 2.4 \times 10^{44} \text{ erg Mpc}^{-3} \text{ yr}^{-1}$, for AGASA and HiRes, respectively.

III. NEUTRINO \rightleftharpoons COSMIC RAY CONNECTION

For optically thin sources, the neutrino power density scales linearly with the cosmic ray power density $\dot{\epsilon}_{\text{CR}}$ [17]. The actual value of the neutrino flux depends on what fraction of the proton energy is converted to charged pions (which then decay to neutrinos). To quantify this, we follow WB and define ϵ_π as the ratio of charged pion energy to the *emerging* nucleon energy at the source. Depending on the relative ambient gas and photon densities, charged pion production proceeds either through inelastic pp scattering [22], or photopion production predominantly through the resonant process $p\gamma \rightarrow \Delta^+ \rightarrow n\pi^+$ [17]. For the first of these, the inelasticity of the process is 0.6 [23]. This then implies that the energy carried away by charged pions is about equal to the emerging nucleon energy, yielding (with our definition) $\epsilon_\pi \approx 1$. For resonant photoproduction, the inelasticity is kinematically determined by requiring equal boosts for the decay products of the Δ^+ [24], giving $\epsilon_\pi = E_{\pi^+}/E_n \approx 0.28$, where E_{π^+} , E_n are the emerging charged pion and neutron energies, respectively.

In this section, we will extend the WB analysis [17] to the case of a lower onset of the extragalactic component. The present analysis differs from WB in that the integrated power spectrum has changed, and that the spectral index $\gamma \neq 2$. We will restrict the ensuing discussion to the case of photopion production on resonance, and comment on the pp possibility at the end of the section.

The intermediate state of the reaction $p + \gamma \rightarrow N + \pi$ is dominated by the Δ^+ resonance. In order to normalize to the observed cosmic rays, we restrict our interest to the $n\pi^+$ decay channel. Each π^+ decays to 3 neutrinos and a positron, $\pi^+ \rightarrow \mu^+ \nu_\mu \rightarrow \nu_\mu \bar{\nu}_\mu \nu_e e^+$. The e^+ readily loses its energy through synchrotron radiation in the source magnetic fields. The average neutrino energy from the direct pion decay is $\langle E_{\nu_\mu} \rangle_\pi = (1-r)E_\pi/2 \approx 0.22E_\pi$ and that of the muon is $\langle E_\mu \rangle_\pi = (1+r)E_\pi/2 \approx 0.78E_\pi$, where r is the ratio of muon to the pion mass squared. Now, taking the ν_μ from muon decay to have 1/3 the energy of the muon, the average energy of the ν_μ from muon decay is $\langle E_{\nu_\mu} \rangle_\mu = (1+r)E_\pi/6 = 0.26E_\pi$. This means that neutrinos carry away about 3/4 of the π^+ energy, and each neutrino carries a fraction $\epsilon_\pi/4$ of the accompanying cosmic ray energy.

In order to correlate the neutrino and cosmic ray fluxes, we assume both follow a common power law at injection

$$\frac{d\dot{N}_i}{dE_i} = C_{\text{CR}(\nu)} E_i^{-\gamma} \quad (4)$$

and normalize our spectrum in a bolometric fashion

$$C_\nu \int_{\epsilon_\pi E_1/4}^{\epsilon_\pi E_2/4} E_i^{-(\gamma-1)} dE_i = \frac{3}{4} \epsilon_\pi C_{\text{CR}} \int_{E_1}^{E_2} E_i^{-(\gamma-1)} dE_i.$$

After integration we have,

$$C_\nu \left(\frac{\epsilon_\pi}{4} \right)^{-(\gamma-2)} = \frac{3}{4} \epsilon_\pi C_{\text{CR}}. \quad (5)$$

Therefore, for the low crossover energy scenario, the resulting flux of neutrinos (all flavors) from optically thin sources is given by [17]

$$J_\nu(E) = 3 \left(\frac{\epsilon_\pi}{4} \right)^{\gamma-1} \frac{\rho_{\text{CR}}}{4\pi} \frac{d\dot{N}_n}{dE_i} \bigg|_{E_i=E} \int_{z_{\text{min}}}^{z_{\text{max}}} \frac{(1+z)^{(n-\gamma)}}{H(z)} dz \\ \sim 3.5 \times 10^{-3} \left(\frac{E}{\text{GeV}} \right)^{-2.54} \text{ GeV}^{-1} \text{ cm}^{-2} \text{ s}^{-1} \text{ sr}^{-1}, \quad (6)$$

where the numerical value is an average flux obtained from best fits to AGASA and HiRes data, derived in Sec. II [25]. This extends the WB analysis to values of $\gamma \neq 2$. The fluxes for each of the best fits are shown in Fig. 3, along with the WB flux. Also shown is the region excluded by AMANDA-B10 for both the cases $\gamma = 2$ and $\gamma = 2.54$, and the cascade limit [26] from Ref. [27], which applies to all scenarios where neutrinos originate from pion decays [28]. For the low crossover scenario, the neutrino flux associated with the AGASA data set is consistent with the AMANDA-B10 data. Sensitivity to this flux will be attained by a full analysis of the AMANDA-II data set [29]. In the event of a positive indication by AMANDA-II, the IceCube facility will (as shown in Sec. V) be capable

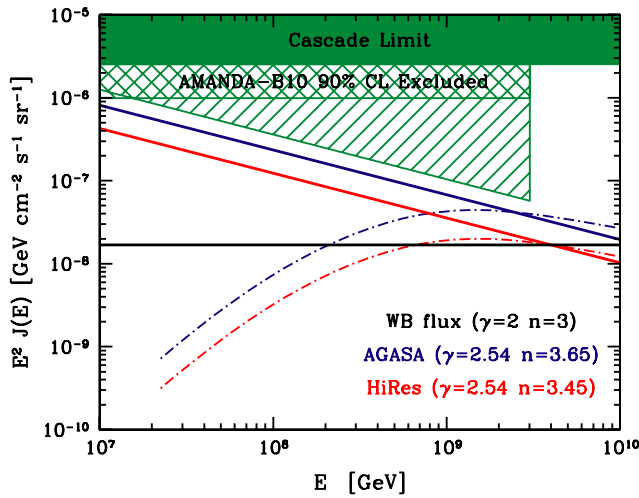


FIG. 3 (color online). Neutrino fluxes (summed over all flavors) from optically thin sources for $\epsilon_\pi = 0.28$. The horizontal solid line indicates the WB prediction which corresponds to a galactic/extragalactic crossover energy at the ankle, $\sim 10^{10}$ GeV. The falling solid lines indicate the expected neutrino flux normalized to HiRes (lower) and AGASA (upper) data, if one assumes the onset of dominance by the extragalactic component is at $10^{8.6}$ GeV. The dash-dotted lines indicate the fluxes of cosmogenic neutrinos associated with flux predictions given by the falling solid lines. The cross-hatched region excludes an E^{-2} spectrum at the 90% CL by measurements of AMANDA-B10 [50]. The single hatched region, obtained by rescaling the AMANDA integrated bolometric flux limit to an $E^{-2.54}$ power law, is the exclusion region for the low crossover model. The shaded region indicates the cascade limit (see text for details).

discriminating between the low and high crossover scenarios.

Several other remarks are in order. (a) The best fit source neutrino fluxes in Fig. 3 correspond to $z_{\min} = 0.012$ and $E_{i,\max} = 10^{12.5}$ GeV. We have checked that a change of z_{\min} to zero and a variation of $E_{i,\max}$ within the range $[10^{11.3}$ GeV, $10^{13.5}$ GeV] produces changes within the order of the thickness of the lines. (b) Because of oscillations, the neutrino flavor mix at the source will evolve to a 1:1:1 mix at the detector [30]. (c) Electron antineutrinos can also be produced through neutron β -decay. However, this contribution turns out to be negligible (about 3 orders of magnitude smaller than the charged pion contribution) [31]. (d) The rapid rise at lower energies of the low crossover neutrino spectrum will greatly increase the event rate at the Glashow resonance as compared to that given in [31] based on the WB flux. The $\bar{\nu}_e$ flux at the Glashow resonance obtained in the low crossover scenario is about an order of magnitude smaller than the bound from AMANDA-II data [32]. (e) Neutrino fluxes from nearby isolated sources (e.g., Centaurus A [22,33] or Cygnus-OB2 [34]) can be distinguished through their point anisotropies, from the differential flux derived in this work.

We now comment on the pp scenario. If the primary proton spectrum $\propto E_i^{-\gamma}$, the dominance of inelastic pp collisions produces an isotropically neutral mix of pions that on decay give rise to a neutrino flux with spectrum $\propto E^{-\gamma}$ [35]. Current hadronic event generators yield an inelasticity of ~ 0.6 [23] for the reaction $pp \rightarrow NN + \text{pions}$, where the N 's are final state nucleons. With our definition, $\epsilon_\pi \approx 1$, assuming that 2/3 of the final state pions are charged. Then, the correction due to a larger inelasticity of pp interactions as compared to the resonant $p\gamma$ scattering (with $\epsilon_\pi \approx 0.28$) would increase the neutrino flux predictions given in Fig. 3 by a factor of ≈ 7 . This sizeable augmentation of the neutrino flux based on optically thin sources with dominant pp scattering will result in the exclusion of the low crossover scenario. Therefore, we will continue to present our results on the basis of the dominance of the photopion process.

IV. COSMOGENIC NEUTRINOS

The opacity of the CMB to ultra-high energy protons propagating over cosmological distances guarantees a cosmogenic flux of neutrinos, originated in the reaction $p + \gamma_{\text{CMB}} \rightarrow N + \pi$ [36]. Very recently, one of us has performed an investigation of the actual size of the cosmogenic neutrino flux [13] assuming that all observed cosmic ray showers above $10^{8.2}$ GeV are initiated by protons, with sources isotropically distributed throughout the Universe. The low energy cutoff used in [13] is near the crossover

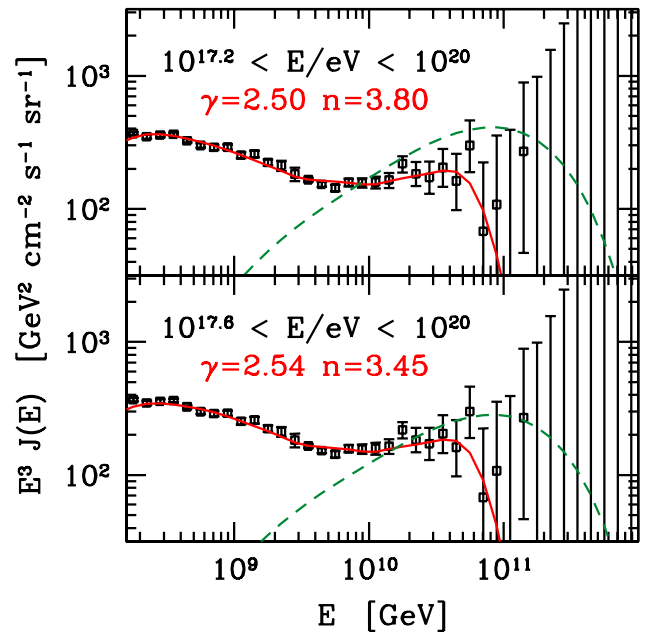


FIG. 4 (color online). Best fit to HiRes data (solid line), assuming dominance of the extragalactic component above $E_- = 10^{8.2}$ GeV (top) and $E_- = 10^{8.6}$ GeV (bottom). Also shown is the associated cosmogenic neutrino flux for all flavors (dashed line).

energy suggested by HiRes data, and thus we expect no significant modification on the prediction of cosmogenic neutrinos. To verify this assertion, we estimate the flux of neutrinos produced as subproducts in the GZK chain reaction by the population of protons that best reproduces the HiRes data. Such a cosmogenic flux is obtained by replacing $P_{p|n}$ in Eq. (1) with $P_{\nu|n}$,

$$J_{\nu} = \frac{1}{4\pi} \int_0^{\infty} dE_i \int_0^{\infty} dr \left| \frac{\partial P_{\nu|n}(E; E_i, r)}{\partial E} \right| \mathcal{L}_n. \quad (7)$$

In Fig. 4 it is seen that the cosmogenic flux predictions for the low energy crossovers at $10^{8.2}$ GeV and $10^{8.6}$ GeV are compatible within errors. It should be noted that the contribution to the cosmogenic neutrino flux resulting from neutron beta decay is negligible for the energies under consideration [37].

The cosmogenic neutrino flux corresponding to the standard E_i^{-2} injection spectrum has been previously obtained in Ref. [37] for several assumed source evolution indices. A comparison with the WB flux shows that these (the cosmogenic and source fluxes) are comparable at energies above 10^8 GeV. This is in striking contrast with the fluxes resulting from the low crossover scenario. As can be seen in Fig. 3, the source flux dominates the cosmogenic flux at energies below 10^9 GeV in the low crossover scenario [38]. Thus, the neutrinos below this energy behave as “unscathed messengers” of the source injection spectrum. The observation of a neutrino flux with a power-law spectral index >2.4 can provide strong support for the low crossover scenario.

V. ICECUBE SENSITIVITY

In the previous sections we have shown that if the nucleon-emitting sources are optically thin, then the diffuse flux of neutrinos produced by these sources provides a powerful tool in discriminating between galactic/extragalactic cosmic ray origin. Should the entire scenario not be ruled out by AMANDA-II data, it is of interest to explore the potential of forthcoming neutrino telescopes to provide conclusive identification of the crossover energy.

In deep-ice/water/salt, neutrinos are detected by observation of the Čerenkov light emitted by charged particles produced in neutrino interactions. In the case of an incident high-energy muon neutrino, for instance, the neutrino interacts with a hydrogen or oxygen nucleus in the deep ocean water (or ice) and produces a muon traveling in nearly the same direction as the neutrino. The blue Čerenkov light emitted along the muon’s kilometer long trajectory is detected by strings of photomultiplier tubes deployed at depth shielded from radiation. The orientation of the Čerenkov cone reveals the neutrino direction. There may also be a visible hadronic shower if the neutrino is of sufficient energy.

The Antarctic Muon And Neutrino Detector Array (AMANDA) [39], using natural 1 mile deep Antarctic ice

as a Čerenkov detector, has operated for more than 3 years in its final configuration of 680 optical modules on 19 strings. The detector is in steady operation collecting roughly four neutrinos per day using fast online analysis software. Its performance has been calibrated by reconstructing muons produced by atmospheric muon neutrinos [40].

Overall, AMANDA represents a proof of concept for the kilometer-scale neutrino observatory, IceCube [18], now under construction. IceCube will consist of 80 km-length strings, each instrumented with 60 10-inch photomultipliers spaced by 17 m. The deepest module is 2.4 km below the surface. The strings are arranged at the apexes of equilateral triangles 125 m on a side. The instrumented (not effective) detector volume is a cubic kilometer. A surface air shower detector, IceTop, consisting of 160 Auger-style [41] Čerenkov detectors deployed over 1 km² above IceCube, augments the deep-ice component by providing a tool for calibration, background rejection and air-shower physics. Construction of the detector started in the Austral summer of 2004/2005 and will continue for 6 years, possibly less. At the time of writing, data collection by the first string has begun.

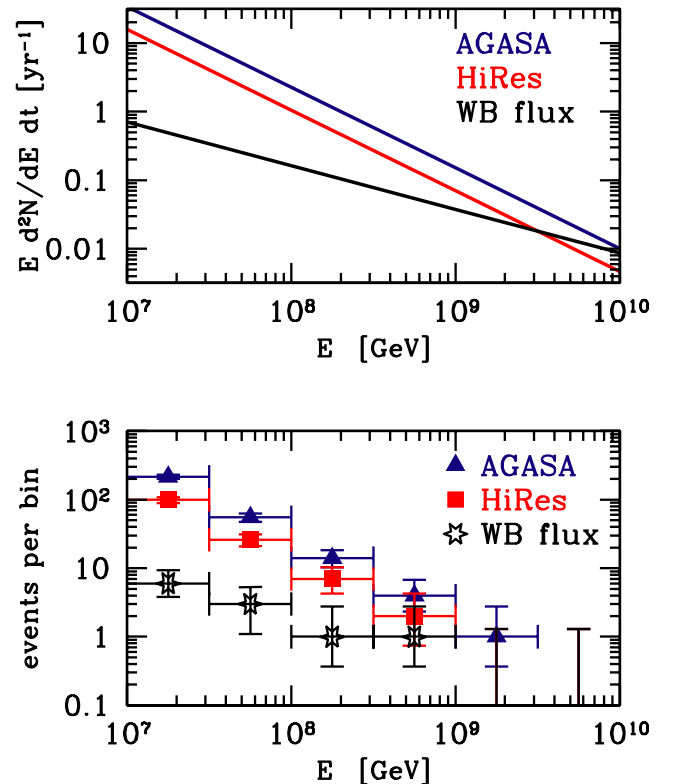


FIG. 5 (color online). Upper panel: Differential event rate at IceCube for the different neutrino flux predictions from AGASA (top), HiRes (middle) and WB (bottom) obtained in Sec. III. Lower panel: Expected bin-by-bin event rates for 10 years of operation. The bin partition interval is taken as $\Delta \log_{10} E = 0.5$.

At the energies under consideration, there is no atmospheric muon or neutrino background in a km^3 detector. The differential event rate is given by

$$\frac{d^2N}{dEdt} \approx 2\pi N_A \rho V_{\text{eff}} J_\nu \sigma_{\nu N}^{\text{CC}}, \quad (8)$$

where N_A is Avogadro's number, $V_{\text{eff}} \approx 2 \text{ km}^3$ is the effective volume of ice with density ρ , and $\sigma_{\nu N}^{\text{CC}} = 6.78 \times 10^{-35} (E/\text{TeV})^{0.363} \text{ cm}^2$ is the charged current neutrino-nucleon cross section [42]. The effective volume used is conservative, since muon tracks can originate well outside the fiducial volume of the detector [43]. In Fig. 5 we show the differential event rate at IceCube from optically thin sources. Also shown are the expected bin-by-bin event rates for 10 years of data collection, with a bin partition size $\Delta \log_{10} E = 0.5$. The vertical error bars are obtained on the basis of Poisson statistics with $\Delta \log_{10} N = 0.434\sqrt{N}/N$, for $N > 20$. For smaller statistics we use Poisson confidence intervals [44]. It is strongly indicated that within its lifetime IceCube will attain sufficient sensitivity to constrain the energy of transition between Galactic and extragalactic dominance. RICE [45], PAO [46], EUSO [47], ANITA [48], and OWL [49] also have the potential to measure the ultra-high energy neutrino flux. However, the energy thresholds, systematics, backgrounds, or time-scales to completion leave these experiments less promising than IceCube for a spectrum determination in the near future.

VI. CONCLUSIONS

We have estimated the extragalactic diffuse neutrino flux emitted from optically thin sources, on the basis of a low transition energy ($10^{8.6} \text{ GeV}$) between galactic and extragalactic cosmic rays. Such a low crossover finds support in the chemical composition analysis of HiRes data [7], and is sustained by studies which reproduce the steepening at the second knee via e^+e^- production on the CMB [11]. Since the neutrino flux reflects the nucleon flux at the source, the latter must be obtained by fitting observed cosmic ray data taking into account propagation effects. The low crossover

energy is well below the threshold energy for resonant $p\gamma_{\text{CMB}}$ absorption, and so samples sources even at large redshift. Thus, source evolution is an important consideration in this calculation. Two-parameter fits in the spectral and redshift evolution indices show that a standard Fermi E_i^{-2} source spectrum is excluded at larger than 95% CL. Best fits to both Akeno [9] & AGASA [2] and Fly's Eye [8,15] & HiRes [4] data sets give an $E_i^{-2.54}$ source spectrum, with an evolution index somewhat larger than 3. The neutrino flux obtained using the WB [17] consideration for energetics at the source mirrors the steep spectrum of the emitted cosmic rays.

Comparison of the resulting flux with existing AMANDA-B10 90% CL bounds [50] reveals the following: (1) If neutrinos are generated by pp interactions at the source, the resulting flux is within the excluded region. (2) For $p\gamma$ interactions dominant, the best fit to the data yields a neutrino flux which is consistent with the AMANDA-B10 upper limit. A complete analysis of the AMANDA data will provide sufficient sensitivity to rule out the model.

The neutrino flux at the source in this scenario dominates the cosmogenic flux. Thus, should data from AMANDA-II not rule out the model, we show that IceCube can measure the characteristic power law of the neutrino spectrum, and thus provide a window on the source dynamics.

In summary, forthcoming data from the South Pole can provide significant clues in demarcating the cosmic ray galactic extragalactic crossover energy.

ACKNOWLEDGMENTS

We would like to thank Birgit Eberle and Yvonne Wong for discussions, and Zoltan Fodor and Sandor Katz for supporting our numerical analysis based on their original computer codes. This work has been partially supported by US NSF (Grant Nos. OPP-0236449, PHY-0140407, PHY-0244507), US DoE (Grant Nos. DE-FG02-95ER40896, DE-FG05-85ER40226), NASA-ATP 02-000-0151, and the Wisconsin Alumni Research Foundation.

-
- [1] See e.g., L. Anchordoqui, T. Paul, S. Reucroft, and J. Swain, *Int. J. Mod. Phys. A* **18**, 2229 (2003).
 [2] M. Takeda *et al.*, *Phys. Rev. Lett.* **81**, 1163 (1998); *Astropart. Phys.* **19**, 447 (2003); AGASA (Akeno Giant Air Shower Array), <http://www-akeno.icrr.u-tokyo.ac.jp/AGASA/24>.
 [3] K. Greisen, *Phys. Rev. Lett.* **16**, 748 (1966); G. T. Zatsepin and V. A. Kuzmin, *Pis'ma Zh. Eksp. Teor. Fiz.* **4**, 114 (1966) [*JETP Lett.* **4**, 78 (1966)].
 [4] T. Abu-Zayyad *et al.* (HiRes Collaboration), *Astropart. Phys.* **23**, 157 (2005).
 [5] N. Hayashida *et al.* (AGASA Collaboration), *Phys. Rev. Lett.* **77**, 1000 (1996); N. Hayashida *et al.* (AGASA Collaboration), *astro-ph/0008102*; G. R. Farrar, *astro-ph/0501388*; See, however, C. B. Finley and S. Westerhoff, *Astropart. Phys.* **21**, 359 (2004).
 [6] R. U. Abbasi *et al.* (HiRes Collaboration), *Astrophys. J.* **610**, L73 (2004); *Astropart. Phys.* **22**, 139 (2004); *astro-ph/0412617*.
 [7] D. R. Bergman (HiRes Collaboration), *Nucl. Phys. B Proc.*

- Suppl. **136**, 40 (2004).
- [8] D. J. Bird *et al.* (Fly's Eye Collaboration), *Phys. Rev. Lett.* **71**, 3401 (1993).
- [9] M. Nagano *et al.*, *J. Phys. G* **18**, 423 (1992).
- [10] T. Abu-Zayyad *et al.*, (HiRes-MIA Collaboration), *Astrophys. J.* **557**, 686 (2001).
- [11] V. Berezhinsky, A. Z. Gazizov, and S. I. Grigorieva, hep-ph/0204357.
- [12] R. U. Abbasi *et al.* (HiRes Collaboration), *Phys. Rev. Lett.* **92**, 151101 (2004); V. Berezhinsky, A. Gazizov, and S. Grigorieva, astro-ph/0302483; V. S. Berezhinsky, S. I. Grigorieva, and B. I. Hnatyk, *Astropart. Phys.* **21**, 617 (2004); V. Berezhinsky, A. Z. Gazizov, and S. I. Grigorieva, *Phys. Lett. B* **612**, 147 (2005).
- [13] Z. Fodor, S. D. Katz, A. Ringwald, and H. Tu, *J. Cosmol. Astropart. Phys.* 11 (2003) 015.
- [14] D. Seckel and T. Stanev, astro-ph/0502244.
- [15] D. J. Bird *et al.* (HiRes Collaboration), *Astrophys. J.* **424**, 491 (1994); **441**, 144 (1995).
- [16] Z. Fodor and S. D. Katz, *Phys. Rev. D* **63**, 023002 (2001); Z. Fodor, S. D. Katz, and A. Ringwald, *J. High Energy Phys.* 06 (2002) 046; Z. Fodor, S. D. Katz, A. Ringwald, and H. Tu, *Phys. Lett. B* **561**, 191 (2003); <http://www.desy.de/~uhec>
- [17] E. Waxman and J. N. Bahcall, *Phys. Rev. D* **59**, 023002 (1999).
- [18] J. Ahrens *et al.* (IceCube Collaboration), *Astropart. Phys.* **20**, 507 (2004).
- [19] E. Waxman, *Astrophys. J.* **452**, L1 (1995); See also, T. K. Gaisser, AIP Conf. Proc. 566 (AIP, New York, 2000).
- [20] A. Mücke, R. Engel, J. P. Rachen, R. J. Protheroe, and T. Stanev, *Comput. Phys. Commun.* **124**, 290 (2000).
- [21] D. N. Spergel *et al.* (WMAP Collaboration), *Astrophys. J. Suppl. Ser.* **148**, 175 (2003).
- [22] L. A. Anchordoqui, H. Goldberg, F. Halzen, and T. J. Weiler, *Phys. Lett. B* **600**, 202 (2004).
- [23] J. Alvarez-Muniz, R. Engel, T. K. Gaisser, J. A. Ortiz, and T. Stanev, *Phys. Rev. D* **66**, 033011 (2002).
- [24] F. W. Stecker, *Phys. Rev. Lett.* **21**, 1016 (1968).
- [25] The derivation of the kernel of integration in Eq. (6) can be obtained using the procedure presented by B. Eberle, A. Ringwald, L. Song, and T. J. Weiler, *Phys. Rev. D* **70**, 023007 (2004).
- [26] V. S. Berezhinsky and A. Yu. Smirnov, *Astrophys. Space Sci.* **32**, 461 (1975).
- [27] K. Mannheim, R. J. Protheroe, and J. P. Rachen, *Phys. Rev. D* **63**, 023003 (2001).
- [28] The cascade limit arises from the requirement that the diffuse gamma-ray fluxes initiated by photons and electrons from pion decays should not exceed measurements. The cascade limit from Ref. [27] exploits the measurement of the diffuse γ ray background by P. Sreekumar *et al.* (EGRET), *Astrophys. J.* **494**, 523 (1998). A lower extragalactic contribution to the γ ray background than that inferred in the above reference, by roughly a factor of 2, has been proposed recently by A. W. Strong, I. V. Moskalenko, and O. Reimer, astro-ph/0306345; U. Keshet, E. Waxman, and A. Loeb, *J. Cosmol. Astropart. Phys.* 04 (2004) 006. The cascade limit may therefore be stronger by a corresponding factor.
- [29] F. Halzen, in XI International Workshop on Neutrino Telescopes, February 2005 (to be published).
- [30] For alternative neutrino oscillation models see e.g., J. F. Beacom, N. F. Bell, D. Hooper, S. Pakvasa, and T. J. Weiler, *Phys. Rev. D* **68**, 093005 (2003).
- [31] L. A. Anchordoqui, H. Goldberg, F. Halzen, and T. J. Weiler, hep-ph/0410003.
- [32] M. Ackermann (AMANDA Collaboration), *Astropart. Phys.* **22**, 127 (2004).
- [33] L. A. Anchordoqui, H. Goldberg, and T. J. Weiler, *Phys. Rev. Lett.* **87**, 081101 (2001).
- [34] L. A. Anchordoqui, H. Goldberg, F. Halzen, and T. J. Weiler, *Phys. Lett. B* **593**, 42 (2004).
- [35] We stress that logarithmic corrections to the spectrum $\propto E^{-\gamma}$ could result in sizeable deviations at very high energy. L. Anchordoqui, H. Goldberg, and C. Nunez, *Phys. Rev. D* **71**, 065014 (2005).
- [36] V. S. Berezhinsky and G. T. Zatsepin, *Phys. Lett. B* **28**, 423 (1969); F. W. Stecker, *Astrophys. J.* **228**, 919 (1979).
- [37] R. Engel, D. Seckel, and T. Stanev, *Phys. Rev. D* **64**, 093010 (2001).
- [38] We have checked that for a change of z_{\min} to zero and for $E_{i,\max}$ larger than the default $10^{12.5}$ GeV, the resulting cosmogenic neutrino fluxes do not change within the energy range shown in Fig. 3. For smaller $E_{i,\max}$, the predicted fluxes get even smaller.
- [39] E. Andres *et al.* (AMANDA Collaboration), *Astropart. Phys.* **13**, 1 (2000).
- [40] E. Andres *et al.*, *Nature (London)* **410**, 441 (2001).
- [41] J. Abraham *et al.* (Auger Collaboration), *Nucl. Instrum. Methods Phys. Res., Sect. A* **523**, 50 (2004).
- [42] R. Gandhi, C. Quigg, M. H. Reno, and I. Sarcevic, *Phys. Rev. D* **58**, 093009 (1998).
- [43] F. Halzen and D. Hooper, *Rep. Prog. Phys.* **65**, 1025 (2002).
- [44] G. J. Feldman and R. D. Cousins, *Phys. Rev. D* **57**, 3873 (1998).
- [45] I. Kravchenko *et al.* (RICE Collaboration), *Astropart. Phys.* **19**, 15 (2003).
- [46] K. S. Capelle, J. W. Cronin, G. Parente, and E. Zas, *Astropart. Phys.* **8**, 321 (1998).
- [47] L. Scarsi, *Nuovo Cimento Soc. Ital. Fis. C* **24C**, 471 (2001); O. Catalano, *Nuovo Cimento Soc. Ital. Fis. C* **24C**, 445 (2001); <http://www.euso-mission.org>
- [48] A. Silvestri *et al.* (ANITA Collaboration), astro-ph/0411007.
- [49] F. W. Stecker, J. F. Krizmanic, L. M. Barbier, E. Loh, J. W. Mitchell, P. Sokolsky, and R. E. Streitmatter, *Nucl. Phys. B Proc. Suppl.* **136C**, 433 (2004).
- [50] M. Ackermann *et al.*, *Astropart. Phys.* **22**, 339 (2005).